Part Four

Strengthening and seismic retrofitting of existing structures: Structural behaviour, design and case studies

Strengthening of existing concrete structures: Concepts and structural behavior

13

T. Triantafillou
University of Patras, Patras, Greece

13.1 Introduction

A number of techniques have been developed that aim at increasing the strength and/or deformation capacity of existing reinforced concrete (RC) structures. These include the use of shotcrete overlays, steel jacketing, externally bonded fiber-reinforced polymers (FRP, such as epoxy-bonded strips or *in situ* impregnated fabrics) and near-surface mounted FRP reinforcement. FRP-based strengthening and/or seismic retrofitting techniques have been well-established in the civil engineering community due to favorable properties offered by these materials. These include high strength and stiffness to weight ratio, corrosion resistance, ease and speed of application and minimal change in the geometry. Despite these advantages over other methods, the FRP strengthening technique entails a few drawbacks, which are mainly attributed to the organic resins used to bind and impregnate the fibers.

The replacement of organic binders with inorganic ones, cement-based polymer-modified mortars, for example, would seem to be the logical course of action. This would target the alleviation of all resin-related problems. Nevertheless, the substitution of FRP with fiber-reinforced mortars would be inhibited by the relatively poor bond conditions in the resulting cementitious composite; due to the granularity of the mortar, penetration and impregnation of fiber sheets is very difficult to achieve. Enhanced fiber–matrix interactions could be achieved when continuous fiber sheets are replaced by textiles. This results in a new generation of materials, which may be thought of as an alternative to FRP in the field of strengthening and seismic retrofitting. These materials have been given the name "textile-reinforced mortar" (TRM) by Triantafillou et al. (2006), "textile-reinforced concrete" (TRC) by German researchers (e.g. Curbach and Jesse, 1999; Brameshuber et al., 2001) and "fabric-reinforced cementitious matrix systems" by ACI (2013). Strictly speaking, the inorganic matrix of textile-based composites is not classified as "concrete," due to the very small size of the aggregates, and does not necessarily contain cement. Hence, the term TRM might be more appropriate.

Textiles comprise fabric meshes made of long-woven, knitted or even unwoven fiber rovings in at least two (typically orthogonal) directions (Figure 13.1). The quantity and spacing of rovings in each direction can be independently controlled, thus affecting the mechanical characteristics of the textile and the degree of penetration

Textile Fibre Composites in Civil Engineering. http://dx.doi.org/10.1016/B978-1-78242-446-8.00014-8

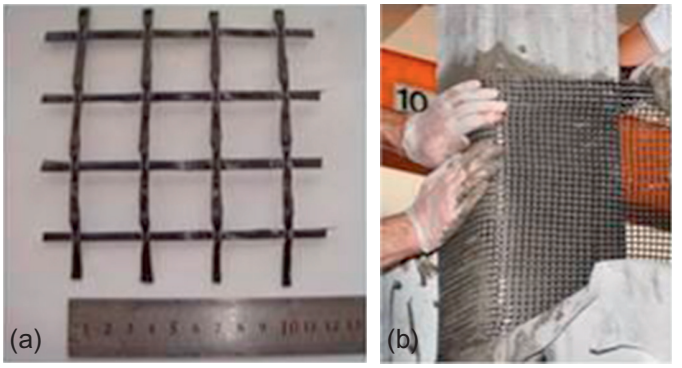

Figure 13.1 (a) Bidirectional textile and (b) application on concrete column.

of the mortar matrix through the mesh openings. The latter is a measure of the composite action achieved for the mortar-grid structure through mechanical interlock. For the inorganic (typically cementitious) matrix (mortar) of externally applied TRM overlays used for strengthening purposes, the following requirements should be met: no shrinkage; high workability (application should be possible using a trowel); high viscosity (application should not be problematic on vertical or overhead surfaces); low rate of workability loss (application of each mortar layer should be possible while the previous one is still in a fresh state) and sufficient shear (hence, tensile) strength in order to avoid premature debonding. Moreover, in cases where E-glass fiber textiles are used, the cement-based matrix should be of low alkalinity.

The TRM system is applied in a way similar to FRP. The concrete is first ground or brushed clean. Then dust and any loose particles are removed (e.g. with air pressure). Finally, a standard wet lay-up procedure is followed to bond the textile layers on the surface of the concrete members. The procedure involves application of the mortar on the (dampened) concrete surface and subsequent application of the textile by hand (Figure 13.1b) and roller pressure. The mortar is also applied in between layers and on top of the last fabric layer. Application of the mortar is made in a few-millimeter (e.g. 3–4 mm) thick layers using a smooth metal trowel. The textile is pressed slightly into the mortar, which protrudes through the perforations between fiber rovings.

This chapter covers basic principles and aspects of the mechanical behavior of RC strengthening with TRM. A number of relevant studies which have provided basic knowledge on the use of TRM as strengthening and seismic retrofitting materials of RC structures are reviewed. In a number of cases, the effectiveness of TRM systems is compared with the one of equivalent FRP systems. The following topics are covered:

- flexural strengthening,
- shear strengthening,
- confinement of axially loaded concrete,
- seismic retrofitting by improving plastic hinge behavior and
- seismic retrofitting of masonry infilled reinforced concrete frames.

13.2 Flexural strengthening

Reinforced concrete elements, such as beams or slabs, may be strengthened in flexure through the use of TRM applied to their tension zones (Figure 13.2). Such reinforcement is not fully effective in the case of beams, as only fibers parallel to the member axis will be activated. Typical load–deflection curves for unstrengthened and strengthened RC beams are compared in Figure 13.3. An increase in the stiffness of the cracked beam can be noted, depending on the amount of axial stiffness added to the beam through the TRM. The increased stiffness limits deflections at the service load level. In terms of cracking, typically more, yet smaller cracks will be observed for the strengthened beam. The yield moment is slightly increased. A considerable increase in the loadbearing capacity is obtained through the additional TRM reinforcement at the expense of a reduction of the ultimate deflection at which the strengthened beam fails. The failure mode often tends to be of a brittle nature, and may typically correspond to debonding between the TRM and the concrete.

A concrete beam strengthened in flexure with externally applied TRM may fail according to the following failure modes: steel yielding followed by concrete

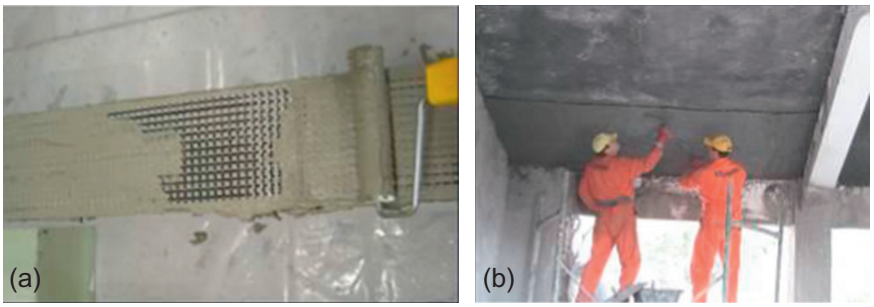

Figure 13.2 Flexural strengthening of (a) beam and (b) two-way slab with TRM.

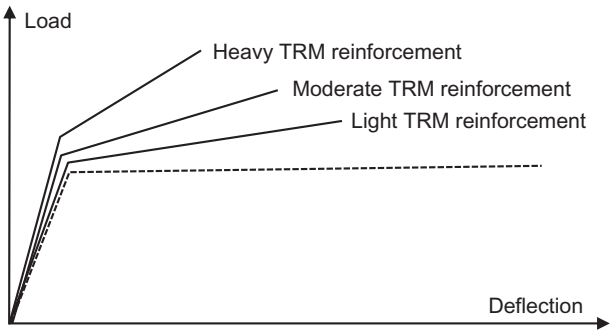

Figure 13.3 Load–deflection curves for different degrees of flexural strengthening.

crushing; steel yielding followed by TRM rupture; concrete crushing (this brittle failure mode is not permitted) and loss of composite action due to debonding, typically after steel yielding (this is the most prevalent failure mode).

In cases where the TRM will reach its design tensile strain before the concrete crushes, failure normally occurs due to debonding rather than rupture. If the mortar in the TRM has shear strength higher than that of concrete, debonding occurs through the concrete, which is the "weak link" in terms of bond capacity. This happens according to one of the following three failure modes: intermediate crack debonding, that is, debonding starting at intermediate cracks; end debonding, that is, failure of end anchorage or concrete cover separation (rip-off). However, if the mortar has relatively low shear strength, debonding will develop due to cracking through the mortar, either between layers of the textile (interlaminar shear failure) or between the first layer of textile and the concrete.

The effectiveness of TRM versus FRP as externally applied flexural strengthening reinforcement of RC *beams* was examined in Triantafillou (2007). The results reported in this study refer to the testing of three under-reinforced beams in four-point bending at a span length of 2.0 m and a shear span of 0.75 m. The beams had a cross section of 150×250 mm and were reinforced with 2Ø12 longitudinal rebars on each side (top and bottom) at a cover of 25 mm. The shear reinforcement comprised Ø8 stirrups at a small spacing of 100 mm to ensure that failure would be controlled by flexural yielding. Self-compacting concrete was used for the casting of the beams with a mean 28-day compressive strength of 34.5 MPa. The steel reinforcement had an average yield stress equal to 530 MPa. The textile comprised equal quantities of carbon fiber rovings in two orthogonal directions with a mass of 168 g/m^2 and a nominal thickness of each layer (corresponding to the equivalent smeared distribution of fibers) equal to 0.047 mm. The mortar had a 28-day compressive and flexural strength of 30.6 and 4.2 MPa, respectively.

One of the three beams was tested without strengthening, as a control specimen (C_fl); a second one was strengthened with four layers of textile bonded with cement-based mortar (M4_fl); and the third beam was identical to the second but with an epoxy resin-based matrix material for the textile reinforcement (R4_fl). The externally bonded reinforcement had a width and a length of 120 mm and 1.90 m, respectively, so that its distance from each support was 50 mm.

The load versus midspan displacement curves for all beams are given in Figure 13.4, which shows that the TRM-strengthened beam (M4-fl) displayed similar characteristics to its FRP counterpart, with some distinct differences: its response was a little more ductile, yielding initiated at a lower load, and the ultimate load was lower. It is believed that these differences are attributed to the lower stiffness of the bond between the external reinforcement and the concrete, which may result in reduced composite action.

The effectiveness of TRM as a measure of increasing the strength and deformation capacity of centrally loaded *two-way slabs* was investigated in Papanicolaou et al. (2009a). To examine this, four slabs cast with perimeter beams (Figure 13.5) were tested under monotonic flexure.

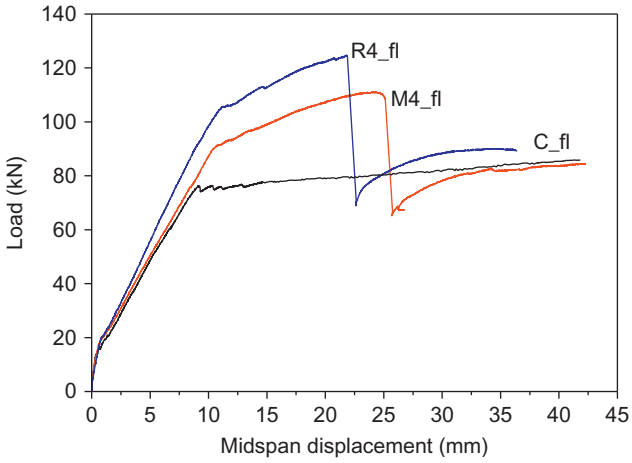

Figure 13.4 Load–displacement response of three simply supported beams strengthened in flexure (Triantafillou, 2007).

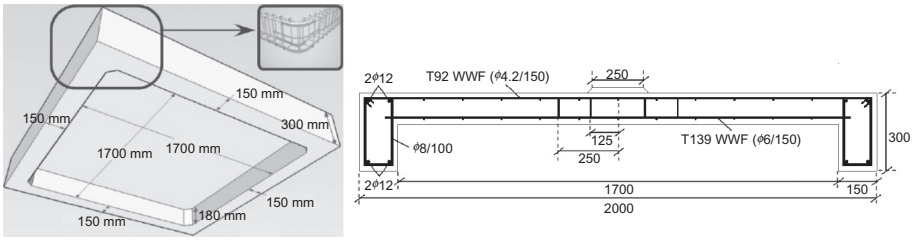

Figure 13.5 Geometry of centrally loaded two-way slabs.

All slabs were fabricated with identical structural steel reinforcement simulating lightly reinforced or, alternatively, moderately corroded slabs. Two welded wire fabrics (WWF) were used: the first comprised a T139 WWF (i.e. 100×100-W13.8 $\times$ W13.8 [mm $\times$ mm-mm^2 $\times$ mm^2]) and was placed at the bottom (tension) surface of the slabs. (The resulting reinforcement ratio was equal to 0.14%.) Whereas the second one was a T92 WWF (i.e. 150×150-W13.8 $\times$ W13.8 [mm $\times$ mm-mm^2 $\times$ mm^2]) and was placed at their top (compression) surface. The slabs were cast using concrete of mean 28-day compressive strength of 25.6 MPa (31.2 MPa at the day of testing). The steel had a conventional yield stress of 645 MPa (at plastic strain 0.2%).

For the specimens receiving TRM overlays, commercial textiles with either carbon or E-glass fiber rovings arranged in two orthogonal directions were used. Both types of textiles shared the same geometry and comprised equal (but different between textiles) quantities of fibers in each direction. The weight of fibers in the textiles was 350 and 500 g/m^2 for the carbon fiber and the E-glass fiber textile, respectively. The nominal thickness of each layer (based on the equivalent smeared distribution

of fibers) was 0.18 mm for both types of textile. The inorganic binder had a 28-day flexural and compressive strength of 6.5 and 24.6 MPa, respectively.

Three specimens were strengthened in total, whereas one served as the control specimen (designated as CON). One specimen received one layer of carbon fiber textile (specimen 1C), another one received two (specimen 2C), whereas the third specimen was strengthened with three layers of E-glass fiber textile (specimen 3G) that had the same axial rigidity (i.e. equal product of fibers' modulus of elasticity and textile thickness) as the single-layered carbon fiber textile (in both directions). These strengthening schemes were selected in this study, so that they would provide useful insight into the effects of the fiber reinforcement ratio and the number of TRM layers (of equivalent axial rigidity).

All specimens were simply supported at their corners on ball-bearing hinges (thus, they were free to rotate at these points) and were subjected to monotonic compressive loading at midspan in a displacement-control mode. The load versus center-point deflection for all specimens is shown in Figure 13.6. All specimens responded in a similar manner in terms of crack development and failure mode. In the uncracked stage, the initial stiffness of all strengthened specimens was higher than that of the control specimen. For all slabs, first cracking due to flexure occurred—as expected—directly below the load application area and at approximately the same load value. With increasing imposed displacement, more flexural cracks formed in both directions along the bars of the tensile steel reinforcement grid (this being more visible in the control specimen). Diagonal cracks were generated propagating from the centers of the specimens to the corners. As recorded by strain gauges, yielding of tensile reinforcement in both directions was delayed in all strengthened specimens.

The failure mechanism involved the sudden punching out of a pyramoid concrete plug at the center of the slabs, accompanied by an immediate and significant drop in

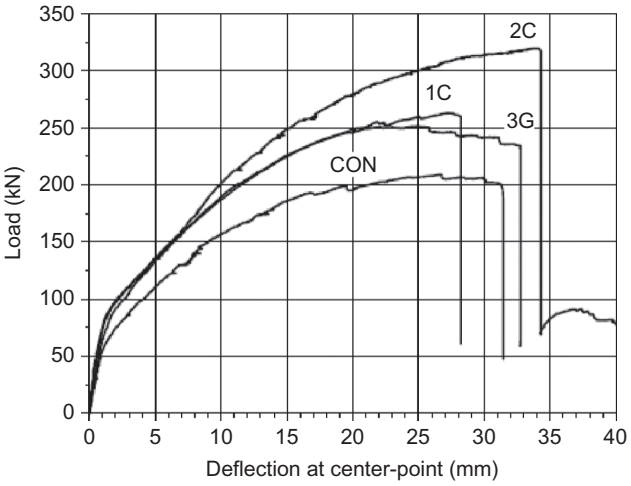

Figure 13.6 Load–center-point deflection curves.

load. Failure was characterized as "flexural punching," as punching occurred shortly after the yielding of the flexural reinforcement (in both directions) near the load application point.

It was concluded in this study that TRM overlays are successful in increasing the load-carrying capacity of flexure-critical RC two-way slabs. Load-carrying capacity increases with increasing fiber reinforcement ratio. Overlays of equal axial rigidity per direction result in a comparable increase of ultimate strength, and interlayer-relative slippage in multilayered systems seems to enhance the deformation capacity of the slabs. Although all strengthened specimens in this study failed due to flexural punching, the failure mode is likely to change to a brittle shear punching should TRM overlays of higher axial rigidity be used. Further details on these test results as well as a comparison with analytical predictions, in good agreement with test results, are given in Papanicolaou et al. (2009b).

13.3 Shear strengthening

The shear capacity of RC members can be enhanced by using TRM jackets, which are activated by bridging shear cracks. Such enhancement is maximized if the TRM forms a closed-force system, for example, by fully wrapping the cross section (Figure 13.7a). Open TRM systems (Figure 13.7b) may also be used for shear strengthening, as long as the reduced effectiveness of the TRM due to debonding is taken into account. Open systems are much more effective when combined with anchorages, as illustrated in Figure 13.7c.

The shear strengthening of beams with rectangular cross sections and *closed jackets* has been investigated by Triantafillou and Papanicolaou (2006). The investigation was carried out on six beams deficient in shear (i.e. with a large spacing of stirrups in the shear span) in four-point bending. The beams measured 2.60 m in length and had a cross section of 150×300 mm. The geometry of the beams, the reinforcement details and the general set-up of the test are shown in Figure 13.8a and b.

The beams were cast using a concrete of mean 28-day compressive strength equal to 30.5 MPa. The steel used for transverse and longitudinal reinforcement had an average yield stress of 275 and 575 MPa, respectively. Textile, mortar, and resin matrices

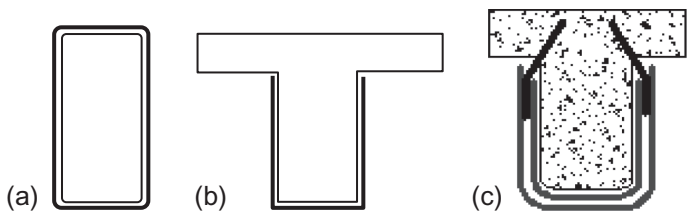

Figure 13.7 Shear strengthening with (a) closed jacket, (b) three-sided jacket, and (c) anchored three-sided jacket.

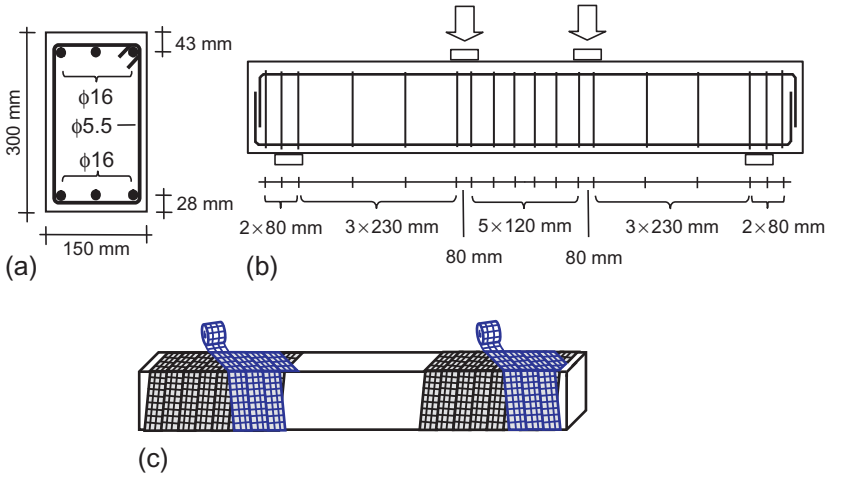

Figure 13.8 (a, b) Geometry of beams and (c) spiral application of strips at the shear spans.

were the same materials as those in the experimental study on flexural strengthening presented in Section 13.2. The influence of three parameters was considered in the experimental investigation: the use of inorganic mortar versus resin-based matrix material for the textile reinforcement, the number of layers (one versus two) and the use of conventional wrapping versus "spirally applied" textiles. Here, "conventional wrapping" corresponds to a single textile sheet being wrapped around the shear span until the desired number of layers is achieved. "Spirally applied" jacketing (Figure 13.8c) was also implemented in one beam and involved the formation of each layer through the use of a single strip, approximately 150-mm wide. The first strip was wrapped around the member in a spiral configuration, starting from one end of the shear span and stopping at the other; the next strip was wrapped in the same configuration but in a direction opposite to that of the first strip. Both strips formed a 10^{o} angle with respect to the transverse to the member axis.

Four of the beams were tested monotonically, and two of them were subjected to cyclic loading. One of the four monotonically tested beams served as a control specimen (C); a second one was wrapped with two layers of mortar-based jacket in the shear span (M2); a third beam was identical to the second, but with a resin-based matrix material for the textile reinforcement (R2); and a fourth beam was strengthened with jackets formed by spirally applied strips (M2-s). The next two specimens were identical to the second and third, but with one layer (instead of two) of textile in a mortar-based (M1) and a resin-based (R1) matrix, respectively. Specimens C, M2, R2, and M2-s were tested monotonically, whereas the remaining two were subjected to quasistatic cyclic loading, all in displacement control. The load versus midspan displacement curves for all specimens are given in Figure 13.9.

The control beam (C) failed in shear, as expected, through the formation of diagonal cracks in the shear spans; the ultimate load was 116.5 kN. No sudden drop in the

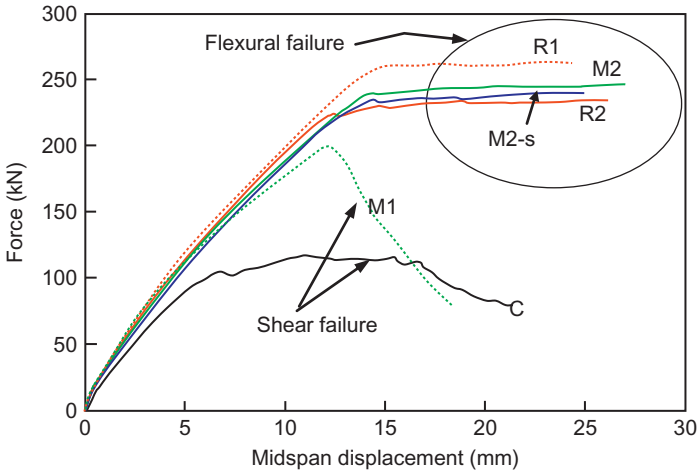

Figure 13.9 Force–midspan displacement curves for all beams tested (for beams M1 and R1 subjected to cyclic loading, the envelope curves in the push direction are given).

load was recorded after diagonal cracking, as considerable contribution to shear resistance was provided by both the stirrups crossing the crack and the strong dowel action (activated by the three Ø16 mm longitudinal rebars).

The behavior of beams R2, M2, M2-s, and R1 indicated that shear failure was suppressed, and that failure was controlled by flexure. Cracks in the constant moment region became wide, and yielding of the tension reinforcement resulted in a nearly horizontal branch of the force versus displacement curve. The maximum loads in specimens R2, M2, and M2-s were 233.4, 243.8, and 237.7 kN, respectively, in other words, nearly the same. This confirms the fact that the shear strengthening scheme selected in this study did not affect the flexural resistance. But the increase in shear resistance was dramatic (more than 100%), regardless of the strengthening scheme. Two layers of textile reinforcement (either in the form of continuous sheets or spirally applied strips) with the cementitious binder performed equally well to the epoxy-bonded (FRP) jacket (with two layers of textile reinforcement). Specimen R1 experienced a flexural yielding failure mode with unequal capacities in the push and pull directions (261.9 and 201.4 kN, respectively). This was possibly due to the unintentionally larger concrete cover at the top of each beam compared to the bottom. Specimen M1 failed in shear (at a peak load of 200.1 kN); this was evident by diagonal cracking in the shear span as well as by the rather sudden strength and stiffness degradation. In this case, the application of a single-layer TRM jacket resulted in a substantial increase in the specimen's shear capacity, with respect to the control specimen, in the order of 70%. It should be noted that for specimen M1: (1) the fracture of the fibers in the cement-based jacket was gradual, starting from a few fiber bundles and propagating slowly in the neighboring fibers and (2) contrary to conventional FRP jackets, beam cracking was clearly visible on the TRM jacket, a feature that facilitates damage assessment.

Overall, it may be concluded that the closed-type TRM jackets employed in this study were quite effective in increasing the shear resistance of RC members. Two layers of textile reinforcement (with a nominal thickness per layer of only 0.047 mm in each of the principal fiber directions) were sufficient to prevent sudden shear failure. Whereas one layer proved less effective compared to its resin-bonded (FRP) counterpart, but still sufficient to provide a substantially increased shear resistance. More details, including modeling aspects, are given in Triantafillou and Papanicolaou (2006).

Shear strengthening of T-beams with *three-sided TRM jackets* has been studied by Brueckner et al. (2006, 2008). A more comprehensive study was carried out by Tzoura and Triantafillou (2014), who investigated experimentally the following parameters not studied before: cyclic loading; fixed support conditions; different types of textiles; different numbers of layers; anchors; the relative performance of TRM versus equivalent FRP systems and different displacement amplitudes of the loading cycles. Tzoura and Triantafillou (2014) tested 13 T-beams as cantilevers (Figure 13.10a) in order to simulate realistic boundary conditions of continuous beams near their supports (columns). All beams were intentionally designed so that their flexural resistance exceeded the shear resistance not only before strengthening but also after, hence only shear failure could develop. Details of beam geometry and reinforcement are given in Figure 13.10b.

For the specimens receiving jacketing (Figure 13.11a), two different textiles ("light" and "heavy") with equal quantities of carbon rovings in two orthogonal directions were used. Each roving was approximately 3-mm wide, and the spacing between rovings (axis-to-axis) was 10 mm. The mass per unit area was 174 g/m^2 for the light textile and 348 g/m^2 for the heavy textile, resulting in a nominal thickness of each layer (based on the equivalent smeared distribution of fibers) of 0.048 and 0.096 mm for the light and the heavy textile, respectively. For the specimens receiving mortar as a binding material, a cementitious dry binder mixed with redispersible polymers was used. The mean compressive and flexural strength of the mortar on the day of testing were 21.8 and 5 MPa, respectively.

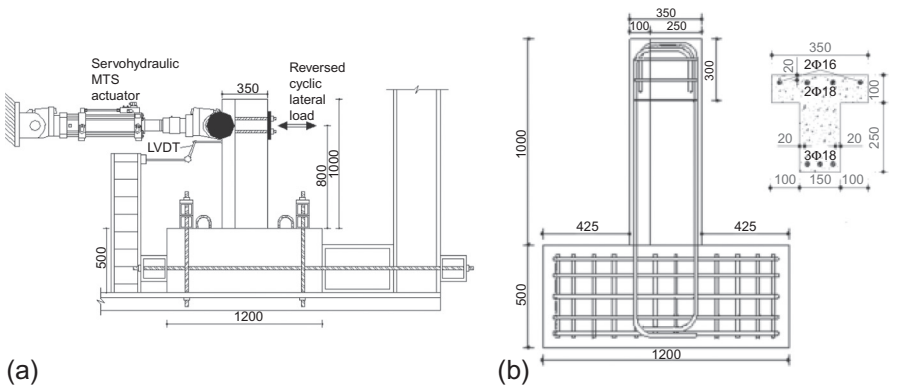

Figure 13.10 (a) Test set-up and (b) beam geometry and reinforcement (dimensions in mm).

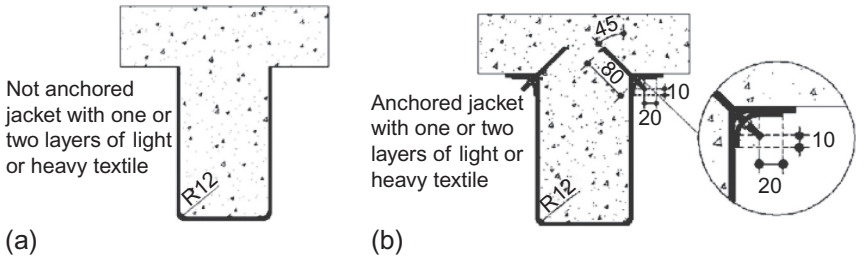

Figure 13.11 Strengthening configuration of the beams tested: (a) U-jackets without anchors and (b) use of anchors.

The anchorage system comprised 3-mm thick curved steel sections fixed at the slab with steel anchors (Figure 13.11b). The steel sections were placed at the corners between the slab and the web, on top of the ends of the jacket, at a radius of 20 mm, while the mortar was still wet. The anchors were made of threaded rods that were 6 mm in diameter; the rods were placed inside 45° holes drilled at a fixed spacing (150 or 100 mm). Holes were drilled into the slab with dimensions of 80 mm in depth and 9 mm in diameter. The holes were filled with a two-part epoxy adhesive to half of their depths, and the anchors were inserted into the holes. Excessive resin was removed, and the steel sections were fixed by tightening the bolts through the use of nuts after hardening of the epoxy adhesive. This method of anchoring was selected on the basis of transferring the tension forces from the jacket into the slab.

All beams were subjected to lateral cyclic loading with a shear span of 0.8 m. Loading comprised successive cycles that progressively increased by fixed amplitudes. The main conclusions from this study are summarized as follows: (a) The effectiveness of TRM jackets without anchorage increases nonproportionally to the number of textile layers. Moreover, for the same total volume fraction of fibers in the jacket, one layer is more effective than two. (b) The anchorage system developed and tested dramatically increases the effectiveness of TRM (and FRP) jackets. (c) Nonanchored FRP jackets are nearly twice as effective as their TRM counterparts. However, if the jackets are anchored, the TRM system is marginally inferior to the FRP system. (d) Modeling of the TRM jacket contribution to the shear resistance of T-beams may be based on the well-known truss analogy, with the stress in the jacket (effective strength) in the range 0.002–0.008, depending on the presence of anchors and their spacing.

13.4 Confinement of axially loaded concrete

In applications where the loading is predominantly static, TRM wrapping may be used in columns to activate a multiaxial state of stress so as to benefit from the commensurate increase in confined concrete strength and deformation capacity. Hence, the axial load capacity will be increased through confinement. The fibers in the hoop direction resist lateral expansion due to compressive stresses in the concrete. This

results in a confining stress to the core, delaying fracture of the concrete and thereby enhancing the compressive strength and the ultimate compressive strain of concrete. This process is significantly more efficient with circular columns than with square or rectangular columns. This is because, with the latter, the confining action is mostly concentrated at the corners, whereas the local strain demand of the TRM jackets increases the risk of localized premature rupture at the corners. Furthermore, similar to FRP, TRM deforms elastically up to very high stresses, and therefore exerts an increasing confining action on concrete until the fibers rupture in the hoop direction.

The effectiveness of TRM versus FRP as a measure of confining axially loaded plain concrete cylinders (150×300 mm, Series A) and short column-type reinforced concrete prisms with a rectangular cross section (200×200 mm, Series B) was reported in Triantafillou et al. (2006) and Bournas et al. (2007), respectively. Each specimen series was cast using the same ready-mix concrete batch (but slightly different from series to series, in terms of water to cement ratio). The steel used for both longitudinal and transverse reinforcement in Series B specimens (Figure 13.12) had an average yield stress of 560 MPa. The four corners of all rectangular prisms were rounded at a radius of 25 mm.

All specimens received textiles as externally bonded reinforcement, except for some of the Series B specimens, in which the epoxy resin-impregnated jackets consisted of fabrics (unidirectional fiber sheets). Specimens are given the notation Y_XN, where Y denotes the series designation (A, B); X denotes the type of jacket—C for the unjacketed/control specimens, M_A for Series A cylinders with mortar jackets, M_B for Series B prisms with mortar jackets (mortar quality in this case being different from mortar M_A) and R for resin-based jackets (FRP); and N denotes the number of layers. Two different commercial unwoven textiles with equal quantities of high-strength carbon fiber rovings in two orthogonal directions were used in these tests. The mass of

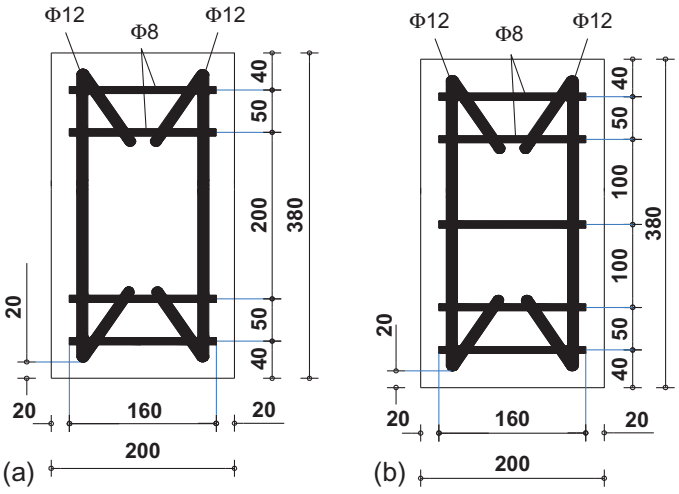

Figure 13.12 Reinforcement configurations for axially loaded RC prisms with stirrups every (a) 200 mm and (b) 100 mm.

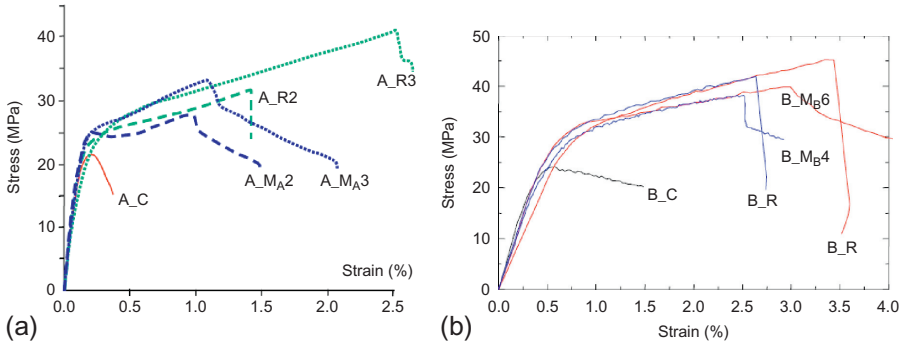

Figure 13.13 Typical stress–strain curves for (a) plain concrete cylinders and (b) RC prisms with stirrups every 100 mm.

fibers in the textile used for all specimens of Series A was 168 g/m^2, and the nominal thickness of each layer (corresponding to the equivalent smeared distribution of fibers) was 0.047 mm. The corresponding values in the textile used in Series B receiving mortar were double (in this case, the rovings were also impregnated with a low-strength polymer). The fabric used for specimens of Series B that were receiving epoxy resin had a unit mass of 300 g/m^2 and a nominal thickness of 0.17 mm. Mortars M_A and M_B were commercial dry polymer-modified, cement-based binders with a 28-day compressive and flexural strength of 30.6 and 4.2 MPa, respectively, for M_A and 22.1 and 6.8 MPa, respectively, for M_B.

Based on the response of all specimens (selected plots are given in Figure 13.13), it is concluded that: (a) TRM confining jackets provide substantial gain in compressive strength and deformation capacity. This gain is higher as the number of confining layers increases. It also depends on the shear strength of the mortar, which determines whether failure of the jacket will occur due to fiber fracture or debonding. (b) Compared with their resin-impregnated counterparts (FRP), TRM jackets may result in a slightly reduced effectiveness, depending on the type of mortar. (c) TRM jackets experienced gradual fracture and a post-peak behavior that was distinctively more compliant than their FRP counterparts, due to the slowly progressing fracture of individual fiber bundles. A more detailed analysis of the results, as well as some modeling aspects of TRM-confined concrete, may be found in Triantafillou et al. (2006) and Bournas et al. (2007).

13.5 Seismic retrofitting by improving plastic hinge behavior

TRM jackets may also be used in plastic hinge confinement (Figure 13.14) of old-type RC columns designed with poorly detailed reinforcement. What matters for earthquake resistance in columns is the compression zone at the ends and, notably, the flexure-controlled ultimate deformation of the member. This ultimate deformation

Figure 13.14 Application of TRM to confine plastic hinge in RC column.

is conveniently expressed by the ultimate curvature (φ_u) of the cross section, which depends heavily on the ultimate strain of the confined concrete ε_{ccu}.

Selected results from the study of Bournas et al. (2007) are presented next. They illustrate a comparison between the increase in ductility provided by TRM jackets and equivalent (i.e. with the same amount of fibers in the circumferential direction) FRP jackets. In this study, three full-scale, identical RC columns were cast using ready-mix concrete with a mean 28-day compressive strength of 25 MPa. The columns measured 1.80 m in height and had a cross section of 250 × 250 mm. Testing was done in a cantilever configuration, with a shear span of 1.60 m. The geometry of the columns, the reinforcement details and the general set-up of the test are shown in Figure 13.15. Details are provided in Bournas et al. (2007). An in-depth experimental investigation for columns with lap-splices is given in Bournas et al. (2011), and the problem of bar buckling is analyzed in Bournas and Triantafillou (2011).

One column was unstrengthened (control specimen); another one received a four-layer TRM jacket in the plastic hinge region (jacket height was equal to 430 mm, accounting for the calculated height of the plastic hinge, Figure 13.14); and a third column was jacketed with two layers of resin-impregnated carbon fiber fabric (FRP). The materials used for jacketing were identical to the ones used for strengthening specimens of Series B in the previously described experimental investigation on confinement of RC prisms. The columns were subjected to lateral cyclic loading under a constant axial load of 460 kN corresponding to 30% of the member's compressive strength. The load versus piston displacement curves for all specimens are given in Figure 13.16.

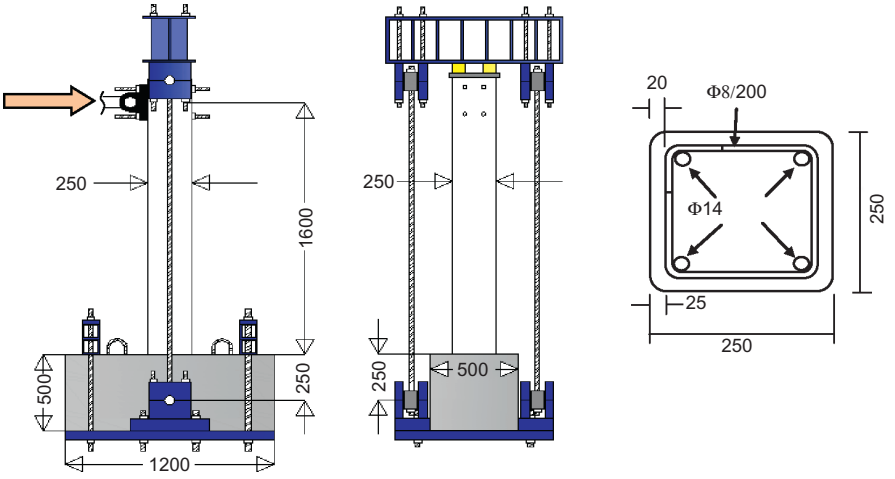

Figure 13.15 Geometry of columns (tested as vertical cantilever) and details of cross section (dimensions in mm).

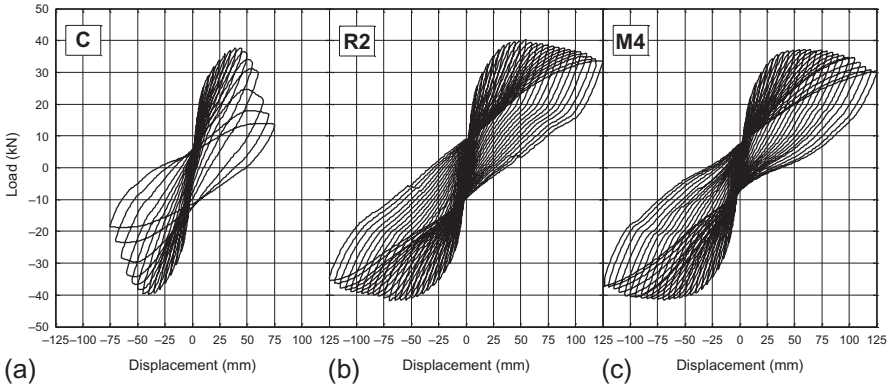

Figure 13.16 Load–displacement curves for (a) the control specimen, (b) the FRP-confined specimen (R2), and (c) the TRM-confined specimen (M4).

The performance and failure mode of all tested columns was controlled by flexure. The concrete cover and part of the core over the lower 200 mm of the unretrofitted column (Figure 13.16a) disintegrated, and bar buckling initiated after the concrete cover spalled off. The behavior of the two retrofitted columns was very similar (Figure 13.16b and c for columns R2 and M4, respectively), but quite different from and far better than their unretrofitted counterpart. Member deformation capacity increased by a factor of more than two; peak resistance was practically the same as in the unretrofitted column; and the post-peak response was quite stable, displaying gradual strength degradation. Although the FRP jacket in column R2 exhibited limited rupture over the lower 50 mm, the TRM jacket remained intact until the test was

Figure 13.17 Pseudodynamic testing of two-story RC building retrofitted at column ends with TRM jacketing.

terminated. When the jackets were removed in both retrofitted columns after the end of the tests, a completely disintegrated concrete core was exposed. It had been kept in place by the heavy confinement provided by the jackets (both FRP and TRM). These tests show that TRM jackets are very effective as a means of increasing the cyclic deformation capacity and the energy dissipation of old-type RC columns with poor detailing, by delaying bar buckling. Compared with equal stiffness and strength FRPs, TRM jacketing has practically the same effectiveness. The high effectiveness of TRM jacketing as a measure of improving plastic hinge behavior was also demonstrated through nearly full-scale testing of a two-story RC building (Figure 13.17), as reported in Bousias et al. (2007).

13.6 Seismic retrofitting of infilled reinforced concrete frames

The contribution of masonry infills to the seismic resistance of existing RC structures is significant, both before separation of the infill from the surrounding frame occurs and during large cycles of imposed deformations near collapse. Strengthening of this type of structure usually aims at increasing the resistance and deformation capacity of the frame itself, setting aside the contribution of infills as a source of strength reserve. An alternative route at improving the performance of existing building structures,

while avoiding the drawbacks of the approach above, is to convert masonry infilling to a more reliable source of resistance by guaranteeing its contribution over the whole spectrum of structural response. This has been examined experimentally and analytically by Koutas et al. (2014a,b). They employed the very promising technique of TRMs on nearly full-scale, as-built and retrofitted three-story masonry infilled frames (Figure 13.18). The frames were subjected to cyclic loading.

Their test results, presented in detail in Koutas et al. (2014a), concluded that: (a) The TRM retrofitting scheme resulted in an enhanced global response of the infilled frame, both in terms of lateral strength and deformation capacity (Figure 13.19). More than a 50% increase in the lateral strength was observed,

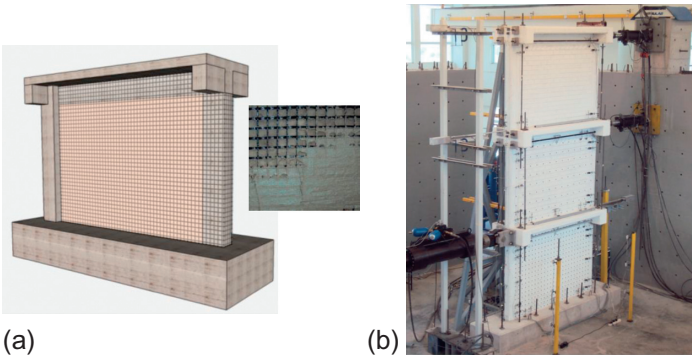

Figure 13.18 Seismic retrofitting of masonry infilled RC frame with TRM: (a) the concept and (b) in-plane testing of three-story frame.

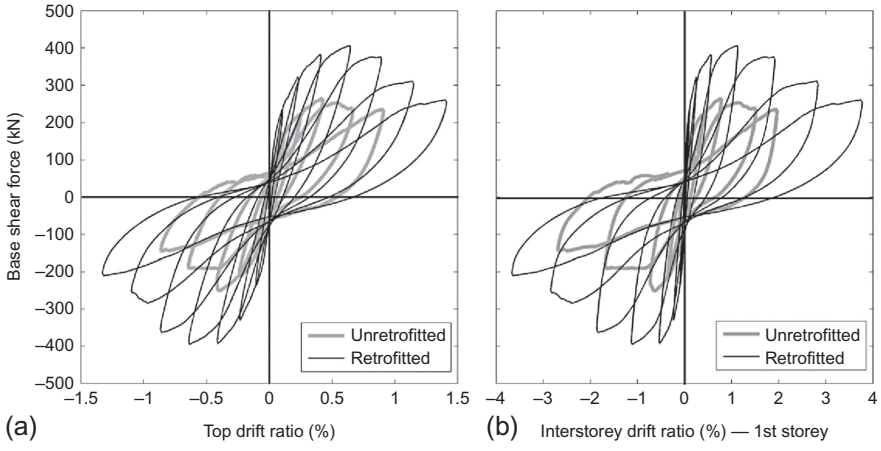

Figure 13.19 Comparative response curves for the two specimens (Sp.#1—unretrofittited and Sp.#2—retrofitted with TRM) in terms of base shear versus (a) top drift ratio and (b) first story drift ratio.

accompanied with more than a 50% higher deformation capacity at the top of the structure at the ultimate strength state. (b) The retrofitted specimen dissipated about 25% more energy than the unretrofitted control for the same loading history. The effect of retrofitting on the lateral stiffness of the first story was an almost twofold increase for low drift levels (up to 0.5%); this became less pronounced at higher drift levels. (c) The height-wise distribution of the lateral story displacements was drastically modified in the retrofitted specimen. Column shear capacity enhancement by TRM wrapping suppressed preemptive column shear failure. This was caused in the control specimen by the lack of adequate transverse reinforcement and the concentration of high shear demands at column end regions, induced by the so-called "diagonal strut." (d) The application of TRM over the entire surface of infills should be supplemented with an adequate infill-frame connection, if a reliable resisting system is to be obtained. For example, this can be done through the use of custom-fabricated, textile-based anchors, which were proved to be particularly effective in delaying or even precluding the debonding of TRM. (e) TRM jacketing proved to be effective in withstanding large shear deformations through the development of a multi-crack pattern and by introducing an efficient load transferring mechanism at the local level. This mechanism is enabled by the capability of the textile itself to distort in shear, while retaining, at the same time, its structural integrity.

An analytical model for describing the behavior of TRM-strengthened masonry-infilled RC frames is introduced in Koutas et al. (2014b), based on the use of a pair of elements per infill diagonal. This simple "macro-modeling" approach was implemented in the *OpenSees* (McKenna et al., 2000) open-source software. It was employed to simulate the response of the three-story masonry infilled RC frame strengthened with TRM and tested under cyclic loading by Koutas et al. (2014a). Model predictions are shown to compare satisfactorily with the experimentally observed response results in terms of the lateral force–displacement response and other response characteristics, such as stiffness and energy dissipation.

13.7 Summary

Fundamental aspects of RC strengthening and seismic retrofitting were presented in this chapter, with a view, in most cases, of comparing the effectiveness of TRM systems with equivalent—in terms of strength and stiffness—FRP ones. The chapter covered: flexural strengthening of RC beams and two-way slabs; shear strengthening of RC beams with rectangular or T-sections, using closed or three-sided jackets, respectively; confinement of axially loaded concrete subjected to concentric compression; seismic retrofitting of columns by improving plastic hinge behavior and seismic retrofitting of masonry infilled reinforced concrete frames. The author demonstrated that, in all cases, TRM jacketing was quite effective—and nearly as effective as FRPs—in improving mechanical performance. This was quantified through strength and/or ductility calculations.

References

ACI 549.4R-13, 2013. Guide to Design and Construction of Externally Bonded Fabric-Reinforced Cementitious Matrix (FRCM) Systems for Repair and Strengthening Concrete and Masonry structures. American Concrete Institute, Farmington Hills, USA.

Bournas, D.A., Triantafillou, T.C., 2011. Bar buckling in RC columns confined with composite materials. J. Compos. Constr. 15 (3), 393–403.

Bournas, D., Lontou, P., Papanicolaou, C.G., Triantafillou, T.C., 2007. Textile-reinforced mortar (TRM) versus FRP confinement in reinforced concrete columns. ACI Struct. J. 104 (6), 740–748.

Bournas, D.A., Triantafillou, T.C., Zygouris, K., Stavropoulos, F., 2011. Bond strength of lap spliced bars in concrete confined with composite jackets. J. Compos. Constr. 15 (2), 156–167.

Bousias, S.N., Spathis, A.-L., Fardis, M.N., Triantafillou, T.C., Papanicolaou, T.C., 2007. Pseudodynamic tests of non-seismically designed RC structures retrofitted with textile-reinforced mortar. In: 8th International Symposium on Fiber-Reinforced Polymer Reinforcement for Concrete Structures—FRPRCS8, Patras, Greece, July 16–18.

Brameshuber, W., Brockmann, J., Roessler, G., 2001. Textile reinforced concrete for formwork elements—investigations of structural behaviour. In: Burgoyne, C.J. (Ed.), FRPRCS-5 Fiber Reinforced Plastics for Reinforced Concrete Structures, vol. 2. Thomas Telford, London, pp. 1019–1026.

Brueckner, A., Ortlepp, R., Curbach, M., 2006. Textile reinforced concrete for strengthening in bending and shear. Mater. Struct. 39 (8), 741–748.

Brueckner, A., Ortlepp, R., Curbach, M., 2008. Anchoring of shear strengthening for T-beams made of textile reinforced concrete (TRC). Mater. Struct. 41 (2), 407–418.

Curbach, M., Jesse, F., 1999. High-performance textile-reinforced concrete. Struct. Eng. Int. 4, 289–291.

Koutas, L., Bousias, S.N., Triantafillou, T.C., 2014a. Seismic strengthening of masonry infilled RC frames with TRM: experimental study. J. Compos. Constr. http://dx.doi.org/10.1061/(ASCE)CC.1943-5614.0000507.

Koutas, L., Triantafillou, T.C., Bousias, S.N., 2014b. Analytical modeling of masonry-infilled RC frames retrofitted with textile reinforced mortar. J. Compos. Constr. http://dx.doi.org/10.1061/(ASCE)CC.1943-5614.0000553.

McKenna, F., Fenves, G.L., Scott, M.H., Jeremic, B., 2000. Open System for Earthquake Engineering Simulation (OpenSees). Pacific Earthquake Engineering Research Center, University of California, Berkeley, CA.

Papanicolaou, C., Triantafillou, T.C., Papantoniou, I., Balioukos, C., 2009a. Strengthening of two-way slabs with textile-reinforced mortars (TRM). In: 11th International fib Symposium, London, June 22–24.

Papanicolaou, C., Triantafillou, T.C., Papantoniou, I., Balioukos, C., 2009b. Strengthening of two-way reinforced concrete slabs with textile reinforced mortars (TRM). In: 4th Colloquium on Textile Reinforced Structures (CTRS4), Dresden, June 3–5.

Triantafillou, T.C., 2007. Textile-reinforced mortars (TRM) versus fibre-reinforced polymers (FRP) as strengthening and seismic retrofitting materials for reinforced concrete and masonry structures. In: International Conference on Advanced Composites in Construction (ACIC07), University of Bath, April 2–4.

Triantafillou, T.C., Papanicolaou, C.G., 2006. Shear strengthening of RC members with textile reinforced mortar (TRM) jackets. Mater. Struct. RILEM 39 (1), 85–93.

Triantafillou, T.C., Papanicolaou, C.G., Zisimopoulos, P., Laourdekis, T., 2006. Concrete confinement with textile reinforced mortar (TRM) jackets. ACI Struct. J. 103 (1), 28–37.

Tzoura, E.A., Triantafillou, T.C., 2014. Shear strengthening of reinforced concrete T-beams under cyclic loading with TRM or FRP jackets. Mater. Struct. http://dx.doi.org/10.1617/s11527-014-0470-9.